Characterization of Spatial Ordering of Corneal Stroma Fibrils

D.E. Freund[1] *P. Burlina*[1, 2] *A. Banerjee*[1]
Johns Hopkins University Applied Physics Laboratory[1] & Computer Science Dept. [2]

ABSTRACT

The quantitative characterization of the cornea's ultrastructure is an important component in clinical studies and ophthalmologic research for investigating various corneal pathologies such as Fuch's dystrophy, bullous keratopathy, and macular corneal dystrophy. The spatial ordering of the stromal fibrils is a good predictor of corneal transparency and light scattering. In this paper this structure is characterized by estimating the probability density function (PDF) associated with some features of the radial distribution function of fibrils seen in electron micrographs of the stroma. A method derived from the Support Vector Data Description (SVDD) is used to estimate this PDF. Experiments using electron micrographs of normal and swollen rabbit corneas are used to illustrate the approach.

Index Terms— PDF estimation, corneal pathologies support vector methods, fibril ordering.

1. INTRODUCTION

The quantitative characterization of the cornea's ultrastructure can play an important role in clinical studies and ophthalmologic research for studying various corneal pathologies. The cornea is the transparent part of the eye's wall having a thickness of approximately 0.5 mm in humans and 0.4 mm in rabbits. The region known as the stroma comprises roughly 90% of the cornea's thickness. The stroma is a layered structure that is made up of many stacked sheets known as lamellae, with corneal cells interspersed between the lamellae making up about 3% to 5% of the total volume of the stroma. As shown in Figure 1, each lamella is composed of long thin collagen fibrils that are embedded in an optically homogeneous ground substance. These fibrils provide the mechanical strength needed to maintain the cornea's curvature [1-6].

In order for normal vision to occur, it is imperative that the cornea maintain its high degree of transparency. One important factor in corneal transparency is the degree of spatial order among the fibrils within the stroma. That is, although the individual fibrils are extremely weak scatterers of light, it has been demonstrated that any degradation in the spatial arrangement of fibrils can result in increased light scattering and hence a loss of transparency [1-6].

Most modern theories of corneal transparency are based on the assumption that the fibrils within the stroma possess some amount of spatial ordering. The assumed degree of spatial order is the primary difference among these theories. For example, Maurice showed that the amount of light scattered from randomly arranged fibrils would be too great for normal vision occur [1]. As a result, he developed a theory in which he assumed perfect long-range crystalline order among the fibrils and showed that this model predicts an amount of light scattering that is in accordance with normal transparency. Since electron micrographs (EM) of corneas do not show the fibrils to be arranged in a perfect crystalline lattice, Maurice had to also assume that the structures seen in EM were artifacts, caused by the preparation of the EM [1-3].

Although EM do not show fibrils arranged in perfect crystalline order they also do not show the fibrils to be arranged randomly. Instead, the fibrils are seen to have what is known as short-range order which is characteristic of the molecular arrangement of fluids. Hart and Farrell showed that the short range order seen in EM can be quantitatively characterized by a radial distribution function, *g(r)* [6-8]. They were also able to show that the short-range spatial order seen in EM was sufficient to reduce the predicted light scattering to be consistent with normal transparency. Subsequently, light scattering experiments have shown that the wavelength dependence of corneal transparency agrees with short-range order as seen in EM [3,4].

Often the loss of transparency seen in diseased or damaged corneas is caused, at least in part, to a disruption in the spatial arrangement of fibrils. We characterize the arrangement of corneal fibrils by computing the PDF of corneal features. In the next section, we illustrate the use of a method derived from SVDD [9,10] to estimate the PDF associated with fibril radial distributions from EMs of freshly excised normal and swollen rabbit corneas. The resulting PDF can be used to effectively discriminate between normal and swollen EMs. An alternate SVM-based PDF estimation approach not pursued here uses regression on the Cumulative Distribution Function as reported in [11].

2. SVDD PDF ESTIMATE

Consider a dataset $\{\mathbf{x}_i,\ i=1,\ldots,N\}$. We seek a kernel-based estimate for the PDF of the data, *f(x),* expressed as a linear mixture of kernels (LMK):

$$f(\mathbf{x}) = \sum_{i=1}^{N} \alpha_i K(\mathbf{x}, \mathbf{x}_i), \qquad (1)$$

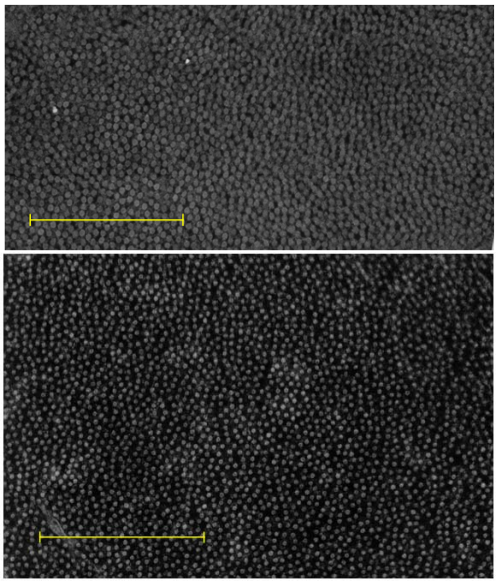

Figure 1 EM cross-section of normal (top) and 15% swollen (bottom) rabbit cornea stromal fibrils with 1 micron scale bar.

where the α_i are non-negative weights that sum to one, and K is a non-negative kernel function which integrates to one.

Before proceeding with the derivation of the density estimator that we will explicitly apply to features derived from corneal EM, we first note that the Parzen estimator is a standard kernel based approach to PDF estimation that, unlike support vector techniques, provides equal weight to each point in the training data. Thus, when $\alpha_i = 1/N$, Eq.(1) becomes the Parzen density estimator [10,12]. However, because all the data are included in the Parzen density estimator, it does not provide a sparse representation for the PDF [10,12]. On the other hand, recent approaches in machine learning such as the support vector machines (SVMs) and relevance vector machines (RVMs) are sparse methods that suggest alternate means of finding the weights α_i to approximate *f(x)*. Here we use an SVM approach known as the Support Vector Data Description (SVDD) for density estimation. While SVDD was originally developed for one-class classification [10], we show here that it can also be used to compute the underlying distribution $f(\mathbf{x})$ in the feature space of the data points $\{\mathbf{x}_i\}$. One advantage that SVDD approach provides is that it can accurately represent arbitrary complex non-Gaussian and multi-modal distributions. More importantly, unlike the Parzen estimator it also provides a sparse computationally efficient representation for $f(\mathbf{x})$ such that most of the α_i are zero.

The SVDD is derived by considering the following geometric problem: find the smallest D-dimensional sphere

$$S = \left\{ \mathbf{x} : \ \| \mathbf{x} - \mathbf{a} \|^2 < R^2 \right\} \quad (2)$$

enclosing the entire set of training exemplars *T*, where:

$$T = \left\{ \mathbf{x_i} \in \mathbb{R}^D, i = 1, .., M \right\}. \quad (3)$$

This constrained optimization problem is solved by defining and then minimizing a Lagrangian. It can be shown that, for the optimal solution, only a small subset of the α_i are non-zero (sparsity), and the center of the sphere **a** is the center of mass of all support vectors which lie at the optimal hypersphere's boundary [10]. The SVDD test statistic is given by the square distance to the boundary:

$$\|\mathbf{x} - \mathbf{a}\|^2 = \langle \mathbf{x}, \mathbf{x} \rangle - 2 \sum_i \alpha_i \langle \mathbf{x}, \mathbf{x}_i \rangle + \sum_{i,j} \alpha_i \alpha_j \langle \mathbf{x}_i, \mathbf{x}_j \rangle \quad (4)$$

where $\langle \mathbf{x}_i, \mathbf{x}_j \rangle$ is an inner product in $\mathbb{R}^D$.

The SVDD test statistic can be generalized to allow for non-spherical support regions by replacing the linear inner-product with a non-linear kernel function $K(\mathbf{x}, \mathbf{y})$. If $K(\mathbf{x}, \mathbf{y})$ is a continuous, symmetric, and positive semi-definite function in L2, then it follows that a mapping, $\Phi(\mathbf{x})$, exists that implicitly maps the training data points from $\mathbb{R}^D$ into a higher (possibly infinite) dimensional induced feature space such that $K(\mathbf{x}, \mathbf{y})$ represents an inner product in this new induced feature space:

$$K(\mathbf{x}, \mathbf{y}) = \langle \Phi(\mathbf{x}), \Phi(\mathbf{y}) \rangle. \quad (5)$$

The SVDD test statistic is then rewritten in terms of the kernel, $K(\mathbf{x}, \mathbf{y})$, as

$$\begin{aligned} SVDD(\mathbf{x}) &\equiv \|\Phi(\mathbf{x}) - \mathbf{c}\|^2 \\ &= K(\mathbf{x}, \mathbf{x}) - 2 \sum_i \alpha_i K(\mathbf{x}, \mathbf{x}_i) + \sum_{i,j} \alpha_i \alpha_j K(\mathbf{x}_i, \mathbf{x}_j) \end{aligned} \quad (6)$$

where **c** is the center of the minimal hypersphere in the induced feature space: $\mathbf{c} = \sum_i \alpha_i \Phi(\mathbf{x}_i)$. It should be noted that, although the SVDD function is a sphere in the induced feature space, in the original feature space it models the support of an arbitrary non-Gaussian, multi-modal function that more accurately captures the distribution of the data.

In this paper, we use a Gaussian radial basis function (RBF) as the kernel function [10]. Since Gaussian RBF satisfy the property that $K(\mathbf{x}, \mathbf{x}) = 1$, the SVDD function simplifies to

$$SVDD(\mathbf{x}) = C - 2 \sum_i \alpha_i K\left(\mathbf{x}, \mathbf{x}_i\right), \quad (7)$$

where C is a constant offset term defined by

$$C \equiv 1 + \sum_{i,j} \alpha_i \alpha_j K\left(\mathbf{x}_i, \mathbf{x}_j\right). \quad (8)$$

$SVDD(\mathbf{x})$ includes a linear mixture of terms comprised of the kernel that we have chosen to model the PDF for the data x_i. Since the α_i are non-negative and sum to one, and the kernel function integrates to one, the right hand side of the SVDD function provides an LMK estimate of the desired PDF given in Eq.(1). Furthermore, since many of the α_i are zero, the SVDD estimate provides a sparse representation that allows for fast evaluation of the underlying distribution. This sparse representation is more amenable to subsequent analysis of the PDF such as

numerically evaluating its value or using optimization to find its modes.

The RBF has one free parameter: the scale parameter σ. This parameter affects the tightness-of-fit for the training data. As explained in [9,10] , it is a measure of how well the SVDD generalizes to unseen data. By varying the scale parameter of the RBF, the SVDD can determine multiple regions of support for a dataset. This allows the SVDD to model non-Gaussian, multi-modal distributions. The estimation of this parameter can be done using various methods including cross validation or minimax [9,10].

3. FEATURE EXCTRACTION

To obtain the features used for SVDD classification and PDF estimation, EM images from both normal and swollen rabbit corneas were analyzed. The magnification of the EMs ranged from ×48,450 to ×53,200 and were scanned at a resolution of 100 μm. A total of thirteen EMs from normal corneas, four EMs from 15% swollen corneas, and three EMs from 25% swollen corneas were used. We followed image analysis algorithms similar to [13] to locate the fibril centers in the EMs. The fibril center data was then used to determine the radial distribution function, *g(r)*, for each EM. We note here that *g(r)* provides a measure of the degree of spatial ordering in liquid like structures [7,8] and thus can be used to determine the amount of fibril ordering in each EM. Specifically, *g(r)* describes how the density of fibrils varies as a function of the radial distance from any given fibril center. That is, let ρ denote the average fibril number density for the entire EM and assume a reference fibril is located at the origin of a local coordinate system. Then the mean fibril density at a distance r from the reference fibril differs from ρ by the factor *g(r)*.

At this point, it is important to recall that any degradation in the spatial ordering of fibrils can cause an increase in light scattering and as a result a decrease in corneal transparency. As just noted, *g(r)* provides a measure of the degree of fibril ordering. Thus, it is reasonable to expect that *g(r)* can be used to distinguish normal (i.e. highly transparent) corneas from abnormal corneas whose transparency is less than normal.

Operationally, the process for determining *g(r)* for an EM is illustrated in Figure 2. Specifically, since an EM has finite extent, one must first choose a maximum distance, r_{max}, over which *g(r)* will be determined and then inscribe a rectangle whose sides are at a distance r_{max} from the corresponding nearest edge of the EM. The number of usable reference fibrils k_c lie inside the rectangle. For each usable reference fibril (e.g. the yellow fibril in Figure 2) a series of "rings" of width *dr* is laid down out to a distance r_{max}. For the kth reference fibril, the number of fibrils in the nth ring, $n_k(r)$, (e.g. the light blue fibrils in Figure 2) is determined and then compared to the mean number, ρA(r) where A(r) is the area of a ring a distance r from the reference fibril. Finally, the results are averaged over the k_c reference fibrils. Therefore *g(r)* can be expressed as

$$g(r) = \frac{\frac{1}{k_c}\sum_{k=1}^{k_c} n_k(r)}{\rho A(r)} \quad (9)$$

In order to increase the number of samples for training and testing, each EM was divided into thirds and *g(r)* was computed for each third of an EM.

A plot of *g(r)* for the EM shown in Figure 2 is given in Figure 3. As indicated in Figure 3, the magnitude and location of the first peak along with the magnitude and location of the first minimum are the four features used for classification and PDF estimation. We have selected these features because the magnitude and location of these maxima and minima are directly correlated to the degree of spatial ordering among the fibrils [7,8].

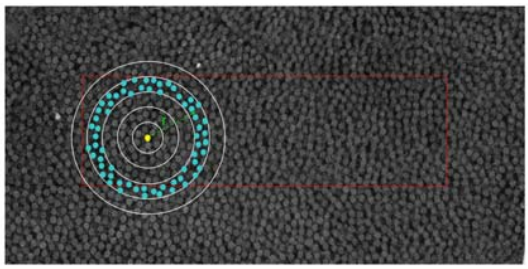

Figure 2 Illustration of how to compute *g(r)* for each EM.

4. EXPERIMENTS

As described in the previous section, *g(r)* was computed for each third of an EM. Dividing the EM into thirds resulted in 39 samples from normal cornea and 21 samples from swollen corneas. Twenty samples from the normal corneas and ten samples from the swollen corneas were used for training. The remaining samples were used for testing.

An RBF kernel function was used with the training data to optimize an SVDD algorithm across the four classification features. This yielded the support of the training data and the corresponding optimal coefficients, α_i. Eq.(1) was used to generate the PDF associated with these optimal coefficients. To illustrate the result, Figure 4 shows the resulting PDF projected into the two dimensional space defined by the (normalized and centered) magnitude of the first maximum and minimum of *g(r)*. The smooth and cross-hatched part of the plot corresponds to the PDF for normal and swollen corneas respectively.

Figure 5 shows the contour plot associated with Figure 4 with the overlap between the two PDFs clearly visible. The solid symbols represent the support vectors obtained when the SVDD algorithm was optimized and the plus signs represent the test data. The green line in Figure 5 is a

decision boundary that is obtained using a likelihood ratio test (LRT) criteria equal to one. When only the two *g(r)* features used to generate Figure 4 and Figure 5 are used for classification, approximately 93% of the test EMs are correctly classified. Provided one can identify the pertinent features, these results are indicative of the level of accuracy obtainable using the SVDD method and shows that it generalizes well to new data. In addition to being a robust method of classification, Figure 4 and Eq.(1) show that SVDD can also be used to associate a probability with any given test vector.

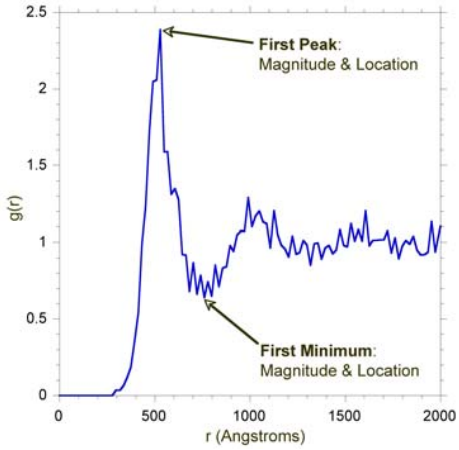

Figure 3 The radial distribution function for the EM shown in Figure 2 with features used for PDF estimation indicated.

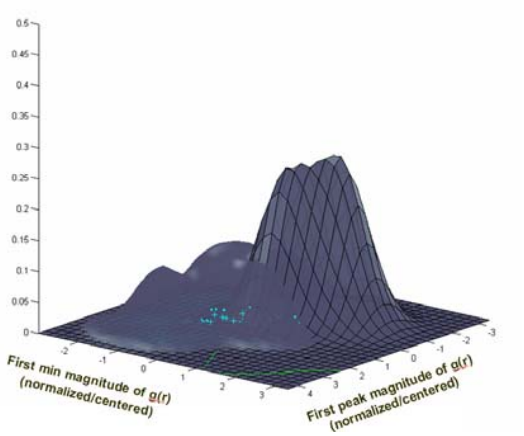

Figure 4 PDF estimation for corneal features

5. CONCLUSION

We use a method derived from SVDD to estimate the PDF associated with features of the radial distribution function to characterize the spatial arrangement of fibrils in the cornea. This distribution has implications for the cornea's optical properties. The sensitivity of this approach is illustrated on rabbit corneal EMs. Using a LRT the PDF is used to correctly discriminate between normal and swollen corneas.

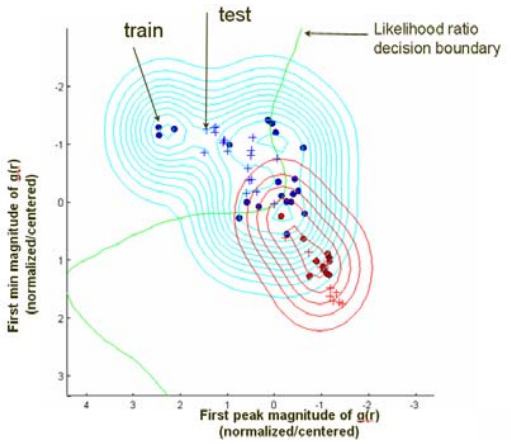

Figure 5 Contour plot of PDF shown in Figure 4. Correct classification is greater than 90%.

REFERENCES

[1] D.M. Maurice, "The Cornea and Sclera" In: H Davson, ed. *The Eye*, Orlando, Fl: Academic Press: 1984;1-158.

[2] D.M. Maurice, "The Structure and Transparency of Corneal Stroma" Journal of Physiology (London) 1957;136:263-285.

[3] R.A. Farrell and R.L. McCally "Corneal Transparency", In: D.M. Albert, F.A. Jakobiec, eds. *Principles and Practice of Ophthalmology 2nd ed*. Philadelphia: WB Saunders; 2000; 629-644.

[4] D.E. Freund, R.L. McCally, R.A. Farrell, "Light-Scattering Tests of Structures in Normal and Swollen Rabbit Corneas", JHU APL Tech. Dig. 1991:12:137-143.

[5] D.E. Freund, R.L. McCally, R.A. Farrell, S.M. Cristol, N.L. L'Hernault, and H.F. Edelhauser, "Ultrastructure in Anterior and Posterior Stroma of Perfused Human and rabbit Corneas", Invest Ophthalmology Vis Sci. 1995:36:1508-1523

[6] R.W. Hart, R. A. Farrell, "Light Scattering in the Cornea",, JOSA, vol. 59:766:774, 1969.

[7] N.K. Ailawadi,"Equilibrium Theories of Simple Liquids", *Physics Reports*,vol 57, 241-306,1980.

[8] J.M. Ziman, *Models of disorder*, Oxford, Cambridge University Press, 1979.

[9] A. Banerjee, P. Burlina and C. Diehl, "A Support Vector Method for Anomaly Detection in Hyperspectral Imagery," *IEEE Trans. Geoscience Remote Sensing*, vol. 8(44), pp. 2282-2291, August 2006.

[10] D.M.J. Tax and R.P.W. Duin, "Data domain description using support vectors," in Proc. *European Symposium on Artificial Neural Networks*, M. Verleysen, editor, pp. 251-256, Brussels, Belgium, April, 1999.

[11] J. Weston, A. Gammerman, M. Stitson, V. Vapnik, V. Vovk, C. Watkins, "Support Vector density Estimation", in Advances in kernel Methods, MIT Press, 1998.

[12] M.P. Wand, M.C. Jones, "Kernel Smoothing", Chapman and Hall, 1995.

[13] D.E. Freund, R.L. McCally, A.D. Goldfinger, R.A. Farrell, "Image Processing of Electron Micrographs for Light Scattering Calculations", Cornea, 466-474, 1993.